

Evolutionary Airfoil Shape Optimization Coupling Parameterization Methods with Lagrangian Vortex Method

Viet Dung Duong^{1*}, Viet Anh Duong²

¹School of Aerospace Engineering, VNU University of Engineering and Technology, Ha Noi, Viet Nam

²University of Science and Technology of Hanoi, Vietnam Academy of Science and Technology, Ha Noi, Vietnam

*Corresponding author email: duongdv@vnu.edu.vn

Abstract

In the present paper, the evolutionary algorithm for single-objective optimization is developed using a genetic algorithm and employing polynomial-based (PARSEC) and radial basis function (RBF) functions for NACA 2412 airfoil parameterization. The determination of the objective functions, being aerodynamic coefficients, are performed using the Lagrangian vortex particle method. The results of the lift coefficient at the wide range of angle of attack using the vortex particle method shows a good agreement with experimental data listed in the literature. For the optimization results, the lift coefficient obtained from the PARSEC method is optimized to be larger for the whole range of angle of attack; while it still keeps the stall region at the upper surface of the airfoil to be the same as that of the original airfoil. In addition, the RBF method illustrates the lift coefficients larger at the range of angle of attack from -5° to 14° but stall occurs earlier than the original airfoil.

Keywords: PARSEC parameterization, single-objective optimization, genetic algorithm, vortex particle method.

1. Introduction

Aviation is currently expanding dramatically all over the world. Therefore, air transportation has become comparable to rail and automotive transport. As a result, massive amounts of carbon dioxide emissions released by aircraft engines increases global warming. In order to reduce these emissions, the aircraft design optimization is required. Aircraft wing shape optimization is today a common method used in the fields of mechanical and aerospace engineering. Aircraft wing aerodynamics design can be divided into two main approaches: Inverse Design (ID) and Direct Number Optimization (DNO). The first method involves finding the wing shape that can respond to fluid dynamics (such as pressure or surface friction distribution); whereas, DNO methods combine geometry definition and aerodynamic analysis code in an iterative process to produce optimal design subject to various constraints.

However, both approaches share the need to modify the wing shape to achieve the goal. Depending on whether the goal is achieved through a small local airfoil modification or a completely new design, different methods of shape parameterization must be employed. Local airfoil shape modifications are usually obtained by smooth perturbations of the original airfoil coordinates through analytical function, such as Legendre, Chebyshev or Bernstein polynomials [1-3]. These methods have the advantage of smooth local modifications, although they have no

direct relation to geometry and this could lead to undulating curves [3].

Historically, the design of the airfoil family requires a parameterized method suitable for each airfoil. Some of the airfoil profile parameters can be found in the literature. An investigation of the parameterization method is referred to as Samareh [4]. Bezier [5, 6] built through the interpolation method as the curves of B-spline. Due to their visualization and flexibility, they have been applied to a wide range of applications with widespread use during shape optimization but caused some problems due to the difficulty in managing the relative position of the control point. Hicks and Henne's [7] gives strong evidence to represent some control points of airfoils, but it is not helpful in designing a new idea. The orthogonal basis function method (OBF method) [8] uses an orthogonal polynomial to describe the upper and lower surfaces of the airfoil, and the shape of the airfoil is determined by five coefficients of the upper surface and lower surface of the airfoil. A commonly used method, which approximates each surface with a sixth-order polynomial, presented by Sobieski [9], is called the PARSEC method. This method uses geometrical properties such as the top position, curvature, and thickness of the airfoil as design variables, allowing for more intuitive shape control. Since this method is limited to only 12 design variables, it does not provide the scope or flexibility in the fidelity offered by many alternatives found in other parts of the aircraft's components. Hence, the multi-

variable-based radial basis function (RBF) can represent nonlinear transformations of the complex geometries [10]. Using these transformations, this method can quickly estimate the output. Nonlinear transformations or mapping functions are determined by equations by solving a linear system. Moreover, the combination of PARSEC parameterization and a genetic algorithms (GA) optimization method to find a Nash equilibrium solution is also performed by Sobieski. Previous optimization processes extensively adopt PARSEC parameterization [11, 12] procedure within GA evolutionary [13, 14]; while the use of RBF has not been employed.

In optimization process, finding the objective functions plays a crucial role in estimating the evident optimized aerodynamic coefficients. The objective functions include games theory [15], grid-based [16] and meshfree methods [17]. To obtain the high accuracy optimization results, the objective functions should satisfy the severe requirements, such as fast computation, high accuracy, easy coupling with parameterization methods. To satisfy those requirements, the meshfree-based vortex particle method is employed in this work [18]. The vortex method simulates external boundary layer flow around complex geometry by tracking local velocities and vorticities of particles, introduced within the fluid domain. The viscous effect is modeled using a core spreading method coupled with the splitting and merging spatial adaptation scheme. The particle's velocity is calculated using the Biot-Savart formulation.

In the present work, we have proposed an evolutionary algorithm based on a genetic algorithm (GA) [19] for optimizing the lift coefficient of an airfoil of aircraft wing employing a polynomial-based (PARSEC) [5] and Radial Basis Function (RBF) [10] shape-parameterized functions. The purpose of the PARSEC function is to parameterize the airfoil family; meanwhile, the RBF function is not only for airfoil shape parameterization but also for other complex shapes of aircraft's component optimization, such as nacelle, winglet, engine, and fuselage. The objective function to find the values of lift and drag coefficients is developed using vortex particle method [18].

In this paper, evolutionary optimization procedures for the aircraft's airfoil family during level flight (low angle of attack) are discussed. That is because in other flight conditions, such as take-off, climb, descend, landing, the level flight condition takes most of the time of economic flight. This optimization process is based on the combination of the GA algorithm with two parameterized methods, PARSEC and RBF to optimize an aircraft's airfoil with the maximized lift. GA is a method of finding an adaptive heuristic search based on genetic principles and natural selection. Similar to organisms that live in nature, GA allows the evolution of a population

according to specific rules of the selection mutation process. Therefore, they move towards maximization of objectives (lift and drag coefficients), as described in Section 1. Next, based on the selectively evolved sample set, Sections 2 and 3 discuss about the parameterization function through the discussion of the PARSEC and RBF parametric methods. Accordingly, the evolutionary solution results are then compared with each other to declare the best fitness shape function for airfoil optimization.

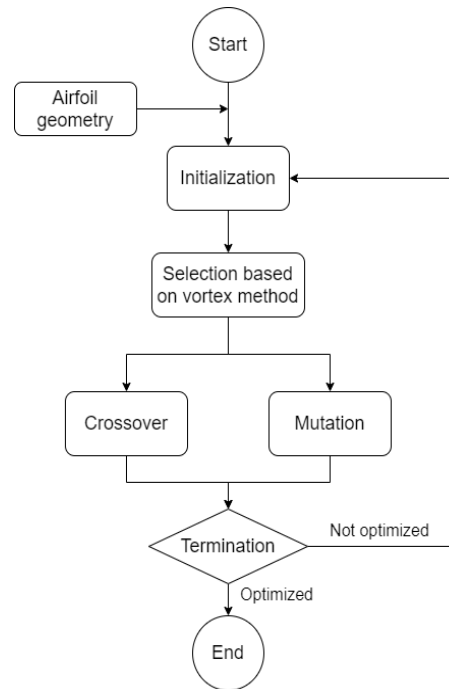


Fig. 1. The evolutionary genetic algorithm

2. Genetic Algorithm

Genetic algorithm (GA) [19, 20] is an evolutionary optimization method based on natural selection that simulates the biological evolution of chromosomes. The algorithm repeatedly modifies the set of individual solutions. Similarly, for the airfoil optimization, at each step, the genetic algorithm randomly selects airfoils from the current population and uses them as parental airfoils to generate child airfoils for the next generation. Through successive generations, the wing profile evolved towards the optimal solution.

In the initialization process, for airfoil configurations, these are parameterized by either the PARSEC and RBF shape function. As those parameters are randomly changed, they create new airfoil generations, which is then intruded into the new population. The new generation of the new airfoil has a closer shape to the airfoil that we are trying to approach the solution. In a selection process, for each airfoil profile, we will find their lift coefficient as an objective function using the vortex panel method

mentioned above. Since then, we can evaluate which configuration of the airfoil has a better lift coefficient.

Genetic operators [21] include the crossover and mutation process. In the crossover, we select two airfoils that we have the corresponding PARSEC and RBF parameters. Then, we select one parameter in the parameter domain and then cross the front-side parameters over the backside parameters of the selected parameter. In mutation, we choose an optional profile from the set created in the initialization process. Then, modify the value of a randomly chosen PARSEC and RBF parameter. In termination, these previous processes are repeated until the end of the program. Possible termination conditions are followings: a solution is found that satisfies minimum criteria; a fixed number of generations is reached; allocated computation time is reached; the optimized solution's fitness is reached or has reached a plateau such that successive iterations no longer produce better results.

3. PARSEC Parameterization

The first idea of parameterizing the airfoil by polynomial function comes from Sobieczky [11]. Initially, this method only used 11 parameters, these parameters were used to determine the geometric shape of the airfoil. In addition, it also includes physical significance, such as leading-edge radius, maximum thickness, trailing edge angles. In this study, we use a subsequently modified 12-parameter PARSEC method [22], which allows the independent determination of the radius of the leading edge, for both the upper and lower surfaces.

Table 1. PARSEC parameters

Parsec parameter	Definition
r_{leup}	Leading edge radius upper surface
x_{up}	Upper crest position in horizontal coordinates
z_{up}	Upper crest position in vertical coordinates
z_{xxup}	Upper crest curvature
r_{lelo}	Leading edge radius lower surface
x_{lo}	Lower crest position in horizontal coordinates
z_{lo}	Lower crest position in vertical coordinates
z_{xxlo}	Lower crest curvature
z_{te}	Trailing edge offset in vertical sense
Δz_{te}	Trailing edge thickness
α_{te}	Trailing edge direction
β_{te}	Trailing edge wedge angle

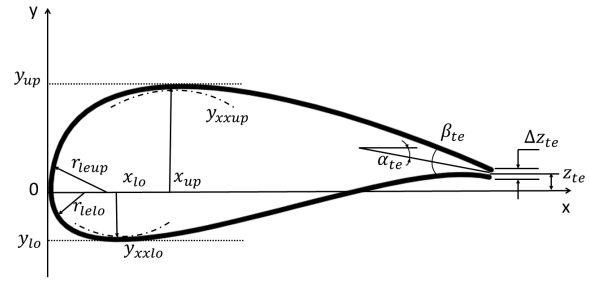


Fig. 2. PARSEC airfoil parameterization with 12 variables expressing the shape of airfoil family.

Fig. 2 and Table 1 show the definitions for the 12 PARSEC parameters. As shown in table 1, a total of 12 variables are used. Fig. 2 illustrates the approach of PARSEC parameterization [22].

Thus, a total of 12 variables are used. The method applied here uses a linear combination of the shape functions to define the upper and lower surfaces [23]. These linear combinations are given by

$$\begin{aligned} \text{Upper: } Z_{up} &= \sum_{i=1}^{n=6} a_{up}^i \cdot x^{i-\frac{1}{2}} \\ \text{Lower: } Z_{lo} &= \sum_{i=1}^{n=6} a_{lo}^i \cdot x^{i-\frac{1}{2}} \end{aligned} \quad (1)$$

where: a_{up}^i and a_{lo}^i are coefficients which are determined by a function of the 12 described geometric parameters, solving two systems of linear equations:

$$\mathbf{Z} = \mathbf{A}\mathbf{X} \quad (2)$$

where:

$$\mathbf{X} = \begin{bmatrix} x_1^{0.5} & x_1^{1.5} & x_1^{2.5} & x_1^{3.5} & x_1^{4.5} & x_1^{5.5} \\ x_2^{0.5} & x_2^{1.5} & x_2^{2.5} & x_2^{3.5} & x_2^{4.5} & x_2^{5.5} \\ \vdots & \vdots & \vdots & \vdots & \vdots & \vdots \\ x_{n-1}^{0.5} & x_{n-1}^{1.5} & x_{n-1}^{2.5} & x_{n-1}^{3.5} & x_{n-1}^{4.5} & x_{n-1}^{5.5} \\ x_n^{0.5} & x_n^{1.5} & x_n^{2.5} & x_n^{3.5} & x_n^{4.5} & x_n^{5.5} \end{bmatrix}$$

$$\mathbf{Z} = \begin{bmatrix} z_1 \\ z_2 \\ \vdots \\ z_{n-1} \\ z_n \end{bmatrix}, \quad \mathbf{A} = \begin{bmatrix} a_1 \\ a_2 \\ \vdots \\ a_5 \\ a_6 \end{bmatrix}$$

The Parsec coefficients can be obtained by transposing and inverting the matrix \mathbf{X} in:

$$\mathbf{A} = (\mathbf{X}^T \mathbf{X})^{-1} (\mathbf{X}^T \mathbf{Z}) \quad (3)$$

Then, the PARSEC parameters are determined by equation (4) to equation (7). The value of x_{up} can be defined by the differential of equation (1). Iterative methods, such as the Newton-Raphson, can be utilized to obtain the value of x_{up} from equation (4):

$$\frac{dz_{up}}{dx} = \sum_{n=1}^6 a_{up,n} (n-0.5)x^{n-1.5} = 0 \quad (4)$$

$$\frac{dz_{lo}}{dx} = \sum_{n=1}^6 a_{lo,n} (n-0.5)x^{n-1.5} = 0$$

The value of z_{up} is determined by substituting the value of x_{up}, x_{lo} obtained in equation (4) into equation (1); then, for a curvature of upper surface, the second differential of equation (1) at the x_{up}, x_{lo} is applied to determine the value of z_{xxup}, z_{xxlo} . The leading edge radius, r_{leup} and r_{lelo} , is simply defined by equation (6) as:

$$r_{leup} = \frac{a_{up,1}^2}{2}, \quad r_{lelo} = \frac{a_{lo,1}^2}{2} \quad (5)$$

Finally, a trailing edge shape is determined by α_{te} and β_{te} :

$$\frac{dz_{up}}{dx} = \sum_{n=1}^6 a_{up,n} (n-0.5) = \tan\left(\alpha_{te} - \frac{\beta_{te}}{2}\right) \quad (6)$$

$$\frac{dz_{lo}}{dx} = \sum_{n=1}^6 a_{lo,n} (n-0.5) = \tan\left(\alpha_{te} + \frac{\beta_{te}}{2}\right) \quad (7)$$

Finally, PARSEC parameters are interpolated back to the linear equations (1). The objective function is determined using the vortex particle method [18] as mentioned hereafter.

4. Radial Basis Function Parameterization

Let us consider the scalar valued function f observed without error, according to the sampling plan $\mathbf{X} = \{x^{(1)}, x^{(2)}, x^{(3)}, \dots, x^{(n)}\}^T$, yielding the responses $\mathbf{Y} = \{y^{(1)}, y^{(2)}, y^{(3)}, \dots, y^{(n)}\}^T$. We seek a radial basis function approximation to \hat{f} of the fixed form.

$$\hat{f}(\mathbf{x}) = \mathbf{w}^T \boldsymbol{\psi} = \sum_{i=1}^{n_c} w_i \psi(\|\mathbf{x} - \mathbf{c}^{(i)}\|) \quad (8)$$

where $\mathbf{c}^{(i)}$ denotes the i^{th} of the n_c basis function centres and $\boldsymbol{\psi}$ is the n_c -vector containing the values of the basis functions ψ themselves, evaluated at the Euclidean distances between the prediction site \mathbf{x} and the centres $\mathbf{c}^{(i)}$ of the basis functions.

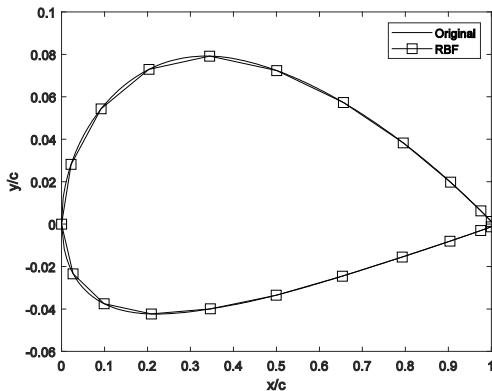


Fig. 3. Airfoil parameterization using radial basis function method.

Thus far, the number of undetermined parameters stands at one per basis function. In this paper, we use the Gaussian-based function ($e^{-r^2/(2\sigma^2)}$). Whether we choose a set of parametric basis functions or fixed ones. The good news is that the term \mathbf{w} is easy to estimate. This can be done via the interpolation condition

$$\hat{f}(\mathbf{x}^{(j)}) = \sum_{i=1}^{n_c} w_i \psi(\|\mathbf{x}^{(j)} - \mathbf{c}^{(i)}\|) = y^{(j)} \quad (9)$$

$$\text{where } j = \overline{1, n_c}$$

Herein lies the beauty of radial basis function approximations. Equation (9) is linear in terms of the basis function weights \mathbf{w} , yet the predictor \hat{f} can express highly nonlinear responses! It is easy to see that one of the conditions of obtaining a unique solution is that the system (9) must be 'square', that is $n_c = n$. It simplifies things if the bases actually coincide with the data points, that is $\mathbf{c}^{(i)} = \mathbf{x}^{(i)}$, $\forall i = \overline{1, \dots, n}$, which leads to the matrix equation:

$$\boldsymbol{\Psi} \mathbf{w} = \mathbf{y} \quad (10)$$

where $\boldsymbol{\Psi}$ denotes the so-called Gram matrix and it is defined as $\boldsymbol{\Psi}_{i,j} = \psi(\|\mathbf{x}^{(i)} - \mathbf{x}^{(j)}\|)$, $i, j = 1, \dots, n$. Since $\boldsymbol{\Psi}$ is a weak matrix, finding \mathbf{w} is very difficult. Hence, we've used the generalized minimal residual method (GMRES) to solve the linear system (10) [24].

5. Vortex Particle Method

The vortex methods are based on the momentum equation and the continuity equation for an incompressible flow which are written in vector form as follows:

$$\frac{\partial \mathbf{u}}{\partial t} + (\mathbf{u} \cdot \nabla) \mathbf{u} = -\frac{1}{\rho} \nabla p + \nu \nabla^2 \mathbf{u} \quad (11)$$

$$\nabla \cdot \mathbf{u} = 0 \quad (12)$$

Taking the *curl* and *divergence* of equation (11) and simplify using equation (12):

$$\frac{\partial \boldsymbol{\omega}}{\partial t} + (\mathbf{u} \cdot \nabla) \boldsymbol{\omega} = (\boldsymbol{\omega} \cdot \nabla) \mathbf{u} + \nu \nabla^2 \boldsymbol{\omega} \quad (13)$$

$$\nabla^2 p = -\rho \nabla \cdot (\mathbf{u} \nabla \mathbf{u}) \quad (14)$$

where \mathbf{u} is velocity vector, p the pressure, and ρ the density. The vorticity $\boldsymbol{\omega}$ is defined as

$$\boldsymbol{\omega} = \nabla \times \mathbf{u} \quad (15)$$

The pressure p can be independently calculated by the Poisson equation (14) once needed. The lagrangian expression for the vorticity transport expressed in equation (13) is then given by

$$\frac{d\boldsymbol{\omega}}{dt} = (\boldsymbol{\omega} \cdot \nabla) \mathbf{u} + \nu \nabla^2 \boldsymbol{\omega} \quad (16)$$

When a two-dimensional flow is dealt with the stretching term, which is the first term on the right-hand side of equation (16), disappears and the two-

dimensional vorticity transport equation is simply reduced to diffusion equation:

$$\frac{d\omega}{dt} = \nu \nabla^2 \omega \quad (17)$$

This equation is solved numerically, by using a viscous splitting algorithm. The algorithm includes two steps. The first step, the so-called convection step, is to track particle elements, containing the certain value of vorticity, with their own local convective velocity by using the Biot-Savart formulation

$$\mathbf{u}(\mathbf{x}, t) = \frac{1}{2} \int \frac{\mathbf{u}(\mathbf{x}', t) \times (\mathbf{x} - \mathbf{x}')}{|\mathbf{x} - \mathbf{x}'|^3} \quad (18)$$

where \mathbf{x} is the position vector. The term inside integral in equation (18) is integrated over all particles within the computational domain.

6. Results and Discussions

The case study in this paper is considered as follows. The NACA 2412 is chosen to be the case because the aerodynamic coefficients are available in the literature. The number of panels of an airfoil is 35. The Reynolds number is set to be 10^6 . The airfoil is stationed and immersed in the computational domain with the 5° angles of attack (AoA). For the inputs of the genetic algorithm, the population size and number of generations to mate are set to be 50 and 40 respectively. The transcendence percentage to choose the group of a dominant airfoil is 5%. Percentages of crossover and mutation process are chosen to be 75% and 20%, respectively. The maximum thickness of the airfoil is constrained to be 0.1 chord length of the airfoil for the convergence of the GA.

Fig. 4 depicts the lift coefficient in the increment of the angle of attack. The in-door code's results, based on the vortex particle method, are in good agreement with experimental results [25] at angle of attack ranging from -5° to 8° . From angle of attack of 10° , a stall occurs at 20° and 16° for present and experimental results, respectively. That is because, at the operating Reynolds number of 10^6 , the inherent vortex blob generation of the vortex method shows a thicker boundary layer compared to the Kolmogorov scale. As a result, the present results at large AoA have deviated from experimental results. Hence, in our optimization algorithm, the AoAs are chosen to be less than 8° . In other words, the AoA is 5° for the lift coefficient optimization in the present work.

Fig. 5 shows the evolution of airfoil based on PARSEC and RBF methods. Fig. 5(a) shows the pressure coefficient distribution on the airfoil surface, and Fig. 5(b) shows the airfoil shapes before and after evolutionary optimization. The diamond dashed line represents airfoil after being evolved by GA with the PARSEC method, while the circle dashed line represents airfoil after the evolution with the RBF method and the squared dashed line stands for the original airfoil. The

PARSEC results show that the pressure coefficients of the lower surface are extended larger than RBF results, while that of the upper surface is lower than RBF results. Accordingly, the pressure coefficients on the upper and lower surfaces of the airfoil are both wider when using both methods compared to that of the original airfoil.

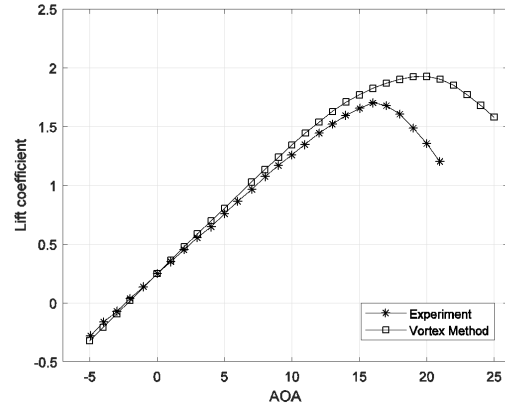
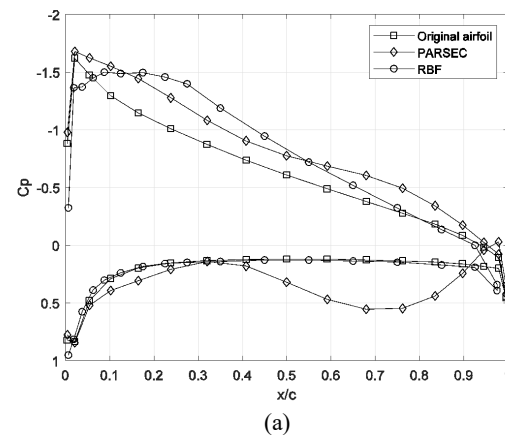
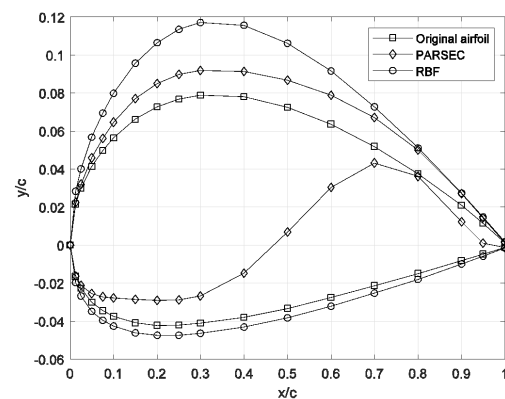


Fig. 4. Lift coefficient versus angle of attack (AoA). Diamond dashed line: the experimental results, star dashed line: the present results



(a)



(b)

Fig. 5. Optimized airfoil by PARSEC and RBF parameterization methods. (a) Pressure coefficient distribution, (b) Airfoil shapes before and after evolutionary optimization

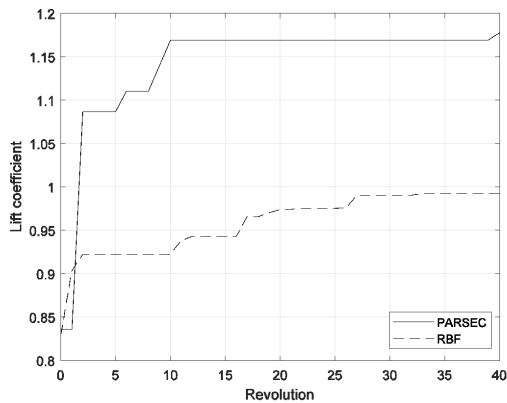


Fig. 6. The evolution of the lift coefficient.

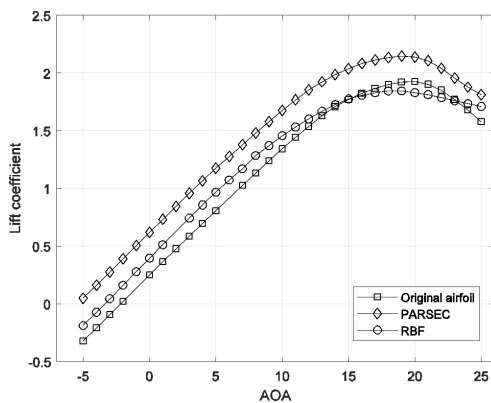


Fig. 7. Lift coefficient versus angle of attack. Diamond, circle dashed lines: the lift coefficient results obtained from PARSEC, RBF parameterization, respectively. Square dashed line: the result of the original airfoil.

Fig. 6 shows an evolution of the lift coefficient using PARSEC and RBF parametric methods. Accordingly, the results obtained from PARSEC and RBF methods have higher lift coefficients than initially when undergoing evolutionary cycles. It can be seen that the PARSEC method gives better lift coefficient results than the RBF method. After 40 evolutionary cycles, the PARSEC method shows the lift coefficient of $Cl = 1.177$ and the RBF method shows the lift coefficient of $Cl = 0.992$.

Fig. 7 depicts the lift coefficient versus the incremental change of AoA. Diamond and circle dashed lines show the lift coefficient results obtained from PARSEC and RBF parameterization, respectively. Square dashed line shows the result of the original airfoil. As demonstrated from the figure, the lift coefficient obtained from the PARSEC method is optimized to be larger for the whole range of AoAs; while it still keeps the stall region at the upper surface of the airfoil to be the same as that of the original airfoil. However, the RBF method illustrates the lift coefficients larger at the range of AoA from -5° to 14° and stall occurs earlier than the original airfoil.

As this result shows, the method of changing the parsec coefficients seems to have significantly increased the lift force coefficient compared with the RBF method when experiencing the same number of evolutionary cycles. However, the reason we use RBF in this case is not only for airfoil evolutionary optimization but also for evolving other complex surfaces often found in aircraft design, such as nacelle, winglet, engine, and fuselage.

For further investigation, we select the angle of attack of 15° to examine the aerodynamic performance of three airfoil designs, including original airfoil of NACA 2412, optimized airfoil using PARSEC parameterization, and optimized airfoil using RBF parameterization. In this case, the Reynolds number is 500 and the grid is applied following the resolution which were carefully examined with direct numerical simulation [18]. Fig. 8 shows the pressure contours (left column) and vorticity contour (right column) of three airfoils. As shown in pressure contour figures, the negative pressure region of PARSEC airfoil on the upper surface is larger than that of original and RBF airfoils. In addition, the positive pressure region of PARSEC airfoil on the lower surface is also larger than that of original airfoil, following the RBF airfoil. This observation is consistent with what was discussed above, where the PARSEC airfoil expresses the excellent optimization of lift coefficient. In the vorticity contour, the boundary layer developed at the upper and lower surfaces seems thinner than that of original and RBF airfoils, thus showing the smaller skin friction drag and larger lift coefficient of PARSEC airfoil.

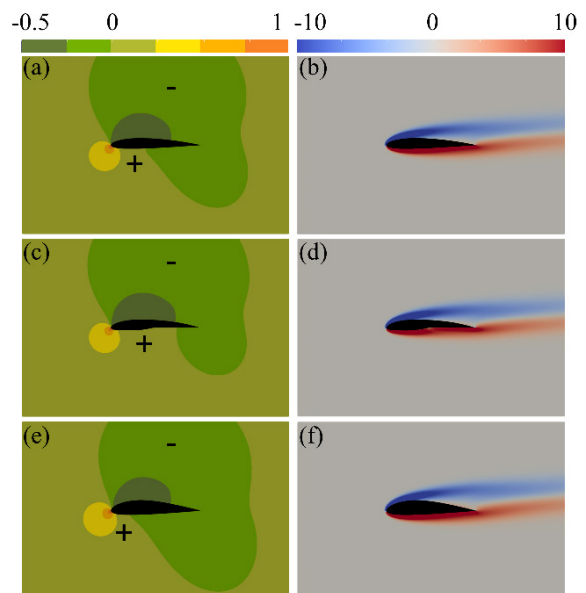


Fig. 8. (a), (c), (e): pressure contours; (b), (d), (f): vorticity contours.

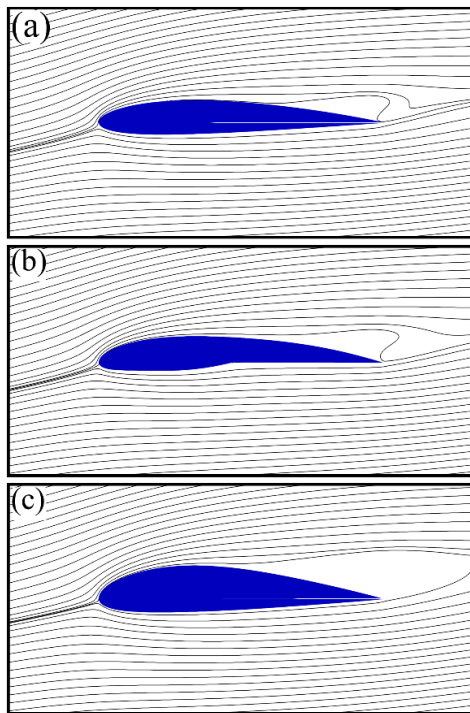


Fig. 9. Streamline contours. (a): original airfoil, (b) : optimized airfoil using PARSEC, (c) : optimized airfoil using RBF.

This can be observed more clearly in Fig. 9, where the wake region of PARSEC and original airfoils is smaller than that of RBF airfoil. It is interesting to note that the separation point on the upper surface of PARSEC airfoil occurs more upstream than that of original airfoil, creating the higher lift coefficient of PARSEC airfoil compared to original airfoil. Furthermore, the separation point of RBF and PARSEC airfoils are nearly the same position. Hence, it is fair to conclude that in order to optimize the lift coefficient of airfoil, the upstream movement of the separation point of the boundary layer on the upper surface plays a significant role.

7. Conclusion

The indoor evolutionary algorithm for single-objective optimization is proposed using a genetic algorithm and employing polynomial-based and radial basis function functions for NACA 2412 airfoil parameterization. The determination of the objective functions (aerodynamic coefficients) are performed using the Lagrangian vortex particle method. The results of the lift coefficient at the wide range of angles of attack using the vortex particle method show a good agreement with experimental data listed in the literature.

For the optimization results, the pressure coefficients on the upper and lower surfaces of the airfoil are both wider when using both methods compared to that of the original airfoil. It is fair to say that the PARSEC method gives better lift coefficient

results than the RBF method. After 40 evolutionary cycles, the PARSEC method shows the lift coefficient of $Cl = 1.177$ and the RBF method shows the lift coefficient of $Cl = 0.992$. The lift coefficients obtained from the PARSEC method are optimized to be larger for the whole range of AoAs, while it still keeps the stall region at the upper surface of the airfoil to be the same as that of the original airfoil. In addition, the RBF method illustrates the lift coefficients larger at the range of AoA from -5° to 14° and stall occurs earlier than the original airfoil.

In the future work, we are going to apply the RBF parameterization method for more complex shapes found in engineering due to its characteristic of highly nonlinear response. In addition, the multi-objective optimization algorithm based on GA is also developed for more objectives in which the optimal engineering designs are always needed.

Acknowledgment

The author would like to thank Research project code USTH.EN.01/23 sponsored by Applied Engineering and Technology Department of University of Science and Technology of Hanoi, VAST for supporting this work.

References

- [1] R. M. Hicks, G. N. Vanderplaats, Application of numerical optimization to the design of low-speed airfoils, NASA TM X-3213, Ames Research Center, Moffet Field, CA, 1975. [online]. Available : <https://ntrs.nasa.gov/citations/19750010109>.
- [2] Q. Ruizhan, Z. Ziqiang, A variable fidelity optimization framework using second-order multi-point additive scaling functions applied to airfoil design, in: 25th International Congress of the Aeronautical Sciences, Hamburg, Germany, 3–8 September, 2006.
- [3] M. Khurana, Airfoil geometry parameterization through shape optimizer and computational fluid dynamics, in: 46th AIAA Aerospace Sciences Meeting and Exhibit, USA, 7th–10th January, 2008. <https://doi.org/10.2514/6.2008-295>
- [4] J. A. Samareh, A survey of shape parameterization techniques, CEAS/AIAA/ ICASE/NASA Langley International Forum on Aeroelasticity and Structural Dynamics, Williamsburg, VA, June 22–25, 1999.
- [5] R. W. Derksen, T. Rogalsky, Bezier-PARSEC: An optimized aerofoil parameterization for design, *Adv.Eng. Softw.*, vol. 41, pp. 923–930, 2010. <https://doi.org/10.1016/j.advengsoft.2010.05.002>
- [6] F. Grasso, Multi-objective numerical optimization applied to aircraft design, PhD thesis, Aerospace Engineering, Department of Aerospace Engineering, University of Naples Federico II, 2008.
- [7] R. M. Hicks, P. A. Henne, Wing design by numerical optimization, *J. Aircr.*, vol. 15(7), pp. 407–412, 1978. <https://doi.org/10.2514/3.58379>

- [8] G. M. Robinson, A. J. Keane, Concise orthogonal representation, *J. Aircr.*, vol. 38(3), pp. 580–583, 2001. <https://doi.org/10.2514/2.2803>
- [9] H. Sobieczky, Parametric airfoils and wings, *Recent Development of Aerodynamic Design Methodologies*, Springer, 1999, pp. 71–87. https://doi.org/10.1007/978-3-322-89952-1_4
- [10] A. Forrester, A. Sobester, A. Keane, *Engineering Design Via Surrogate Modelling: A Practical Guide*, John Wiley & Sons, 2008. <https://doi.org/10.1002/9780470770801>
- [11] H. Sobieczky, Geometry generator for CFD and applied aerodynamics, in: *Courses and Lecture International*, 1997. https://doi.org/10.1007/978-3-7091-2658-5_9
- [12] H. Sobieczky, Parametric airfoils and wings, in: K. Fujii, G.S. Dulikravich (Eds.), *Notes on Numerical Fluid Mechanics*, vol. 68, pp. 71–88, 1998. https://doi.org/10.1007/978-3-322-89952-1_4
- [13] E. Makoto, Wind turbine airfoil optimization by particle swarm method, Ms.D. thesis, Department of Mechanical and Aerospace Engineering, Case Western Reserve University, 2011.
- [14] M. Y. V. Pehlivanoglu, Representation method effects on vibrational genetic algorithm in 2-D airfoil design, *J. Aeronaut. Space Technol.*, vol. 4 (2), pp. 7–13, 2009.
- [15] D. Vecchia, Pierluigi, E. Daniele, and E. D’Amato., An airfoil shape optimization technique coupling PARSEC parameterization and evolutionary algorithm, *Aerospace Science and Technology*, vol. 32(1), pp. 103-110, 2014. <https://doi.org/10.1016/j.ast.2013.11.006>
- [16] C. B. Allen, D. J. Poole, and T. C. Rendall, Wing aerodynamic optimization using efficient mathematically-extracted modal design variables, *Optimization and Engineering*, vol. 19, pp. 453-477, 2018. <https://doi.org/10.1007/s11081-018-9376-7>
- [17] R. Mukesh, K. Lingadurai, and U. Selvakumar, Airfoil shape optimization using non-traditional optimization technique and its validation, *Journal of King Saud University-Engineering Sciences*, vol. 26(2), pp. 191-197, 2014. <https://doi.org/10.1016/j.jksues.2013.04.003>
- [18] D. V. Dung, L. R. Zuhail, H. Muhammad, Two-dimensional fast Lagrangian vortex method for simulating flows around a moving boundary, *Journal of Mechanical Engineering*, vol. 12(1), pp. 31-46, 2015.
- [19] S. Koziel, X. S. Yang, *Computational Optimization, Methods and Algorithms*, 2011, pp. 19-20. <https://doi.org/10.1007/978-3-642-20859-1>
- [20] K. F. Man, K. S. Tang, S. Kwong, *Genetic Algorithms : Concepts and Designs*, 1999. <https://doi.org/10.1007/978-1-4471-0577-0>
- [21] P. D. Vecchia, E. Daniele, E. D’Amato, An airfoil shape optimization technique coupling PARSEC parameterization and evolutionary algorithm, *Aerospace Science and Technology*, vol. 32, pp. 103-110, 2014. <https://doi.org/10.1016/j.ast.2013.11.006>
- [22] K. Slawomir, X. S. Yang, *Computational optimization: An overview. Computational Optimization, Methods and Algorithms (2011): 1-11.*
- [23] S. Jung, W. Choi, L. S. Martins-Filho, F. Madeira, An implementation of self-organizing maps for airfoil design exploration via multi-objective optimization technique, *Journal of Aerospace Technology and Management*, pp. 193-202, 2016. <https://doi.org/10.5028/jatm.v8i2.585>
- [24] Y. Saad, M. H. Schultz GMRES: A generalised minimal residual algorithm for solving nonsymmetric linear systems, *SIAM Journal of Scientific Computing*, vol. 7(3), 1986. <https://doi.org/10.1137/0907058>
- [25] Abbott, I. H., and A. E. von Doenhoff: *Theory of Wing Sections*, Dover Publications, Inc., New York, 1959.